

Embedding protein 3D-structures in a cubic lattice.

I. The basic algorithms.

Jacques Gabarro-Arpa

LBPA CNRS, Ecole Normale Supérieure de Cachan

61, Avenue du Président Wilson - 94235 Cachan cedex - France

e-mail: jga@gtran.org

Abstract

Realistic 3D-conformations of protein structures can be embedded in a cubic lattice using exclusively integer numbers, additions, subtractions and boolean operations.

1. Introduction

In previous papers [1 – 5] we have built a series of mathematical tools for studying the multidimensional molecular conformational space of biological macromolecules, with the aim of understanding the dynamical states of proteins by building a complete energy surface [6, 7].

An N -atom molecule has a $(N-1)^3$ -dimensional conformational space (CS), the sheer complexity of this huge structure can be reduced to tractable dimensions by partitioning it with central hyperplanes¹ into a finite set of cells, this amounts to discarding all knowledge about molecular conformations other than the cells that contain them.

In our approach [1], a set \mathcal{H} of $N_{\mathcal{H}} = N \times (N-1)/2$ hyperplanes generates a partition in CS of $N!^3$ cells, on the other hand hyperplanes are oriented structures dividing the space into a $+$ and a $-$ half-spaces, thus points within a cell are characterized by a binary sequence of length $N_{\mathcal{H}}$ enumerating the orientations with respect the hyperplane set. This binary sequence is all the information that remains from the molecular conformations.

Our choice of hyperplanes $\{H_{ij} \in \mathcal{H} : c_i - c_j = 0, \quad 0 \leq i < j \leq N-1, \quad c \in \{x, y, z\}\}^2$ [1], is such that the $+/ -$ hemispaces are the points with $c_i > c_j$ and $c_i < c_j$ respectively. This induces an order relation in the x , y and z coordinates of points in a cell

$$c_{\alpha_0} < c_{\alpha_1} < c_{\alpha_2} < \dots < c_{\alpha_{N-2}} < c_{\alpha_{N-1}} \quad (1)$$

where $\{\alpha_0, \alpha_1, \alpha_2, \dots, \alpha_{N-2}, \alpha_{N-1}\}$, a permutation of the sequence $\{0, 1, 2, \dots, N-2, N-1\}$, is the **dominance partition sequence** (DPS)[1].

¹That pass through the origin.

²A convention used here is that c represents any of the cartesian coordinates x , y , z .

The compactedness and hierarchical structure of the codes generated by partition sequences made possible the construction of a graph whose nodes are the cells in CS that are visited by the thermalized molecule with edges towards adjacent cells, this was the subject developed in previous works [2 – 5].

However interesting this result may be, it is of no practical use unless on top of it there is a method for calculating the energy of molecular conformations in a cell. With the mesoscopic force field approximations currently used in molecular simulations [8, 9], where atoms are represented as point-like structures, the only input to the Hamiltonian energy function are the interatomic distances calculated from 3D molecular conformations. In this framework the purpose of this work is twofold:

1. given a partition sequence, we want to calculate a fair sample of compatible 3D molecular conformations,
2. we want to encode the set of sampled conformations with a combinatorial structure so they can be more easily manipulated.

In the following sections are described the algorithms for doing this:

- In section 2 we build a complete set of lattice covalent bond segments, which are the basic building blocks: the whole molecular structure is built upon them.
- The *DPS*s can be seen as the lattice projections of a molecular structure where all intervals in each dimension are reduced to one lattice spacing (Fig. 5 of [1]), these have to be increased locally to obtain a realistic structure. In section 3 we build the partially ordered set of lattice intervals between bonded atoms, a structure needed for calculating the maximum and minimum expansion values of each interval, this gives a set of linear inequalities described in section 4.
- In section 5 it is shown how an inter-dependent system of inequalities can be made independent.
- In section 6 the form and structure of the system of linear inequalities is discussed in detail.

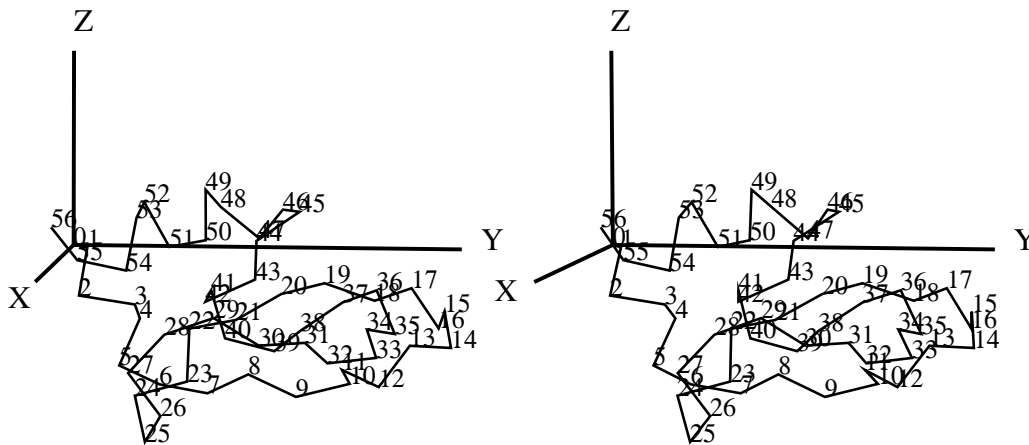


Figure 1: Stereoview of a *pancreatic trypsin inhibitor protein* (PTI) C_α -backbone molecular conformation (Table I), corresponding to the dominance partition sequences in Fig. 2.

To illustrate the algorithmic methods that are the subject of the present work, we have chosen as an example (Fig. 1 and Table I) the C_α -backbone of the pancreatic trypsin inhibitor protein [10], because it is a small protein molecule and the mathematical structures it generates are of moderate size, yet it has the complexity that can be found in longer molecules. Also the side chains have been put aside for the same reason: they would have made the contents of Figs. 2 and 3 almost unreadable.

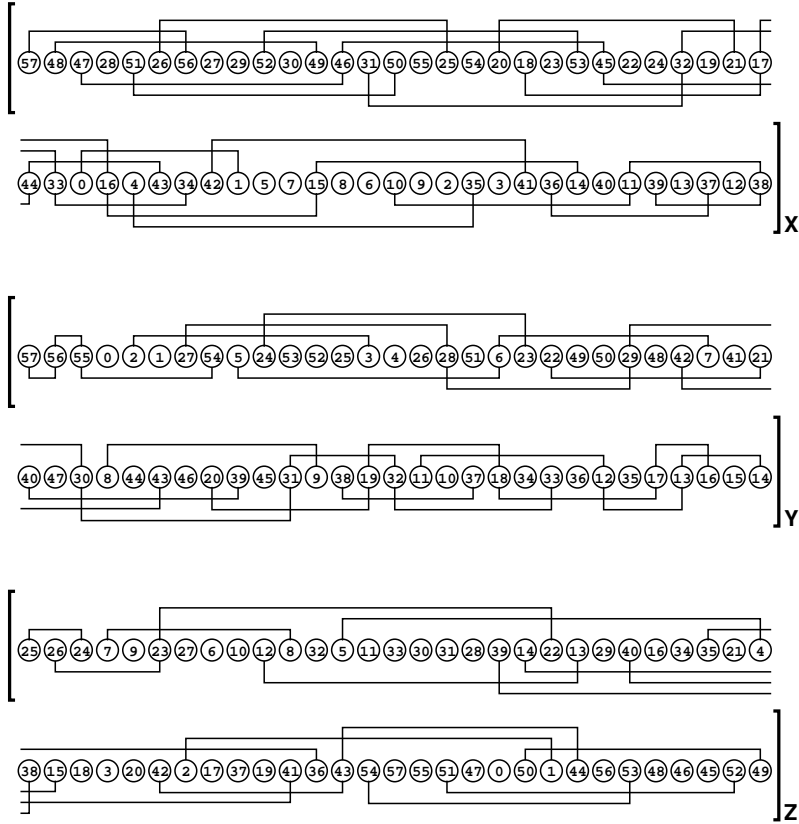


Figure 2: Dominance partition sequence of the *PTI* C_α -backbone for the molecular conformation from Fig. 1. Showing the maximal intervals for each coordinate.

2. The expanded lattice covalent bond segments set

The numbers in x , y and z dominance partition sequences can be regarded as the evenly spaced projections of N points in a $3D$ cubic lattice, it is a particular form of embedding where the separation between consecutive projections of atoms in x , y and z has been shrunk to one lattice spacing. The aim of the present work is to expand this embedding so to obtain realistic molecular structures.

To do this we must restrict the most basic element of molecular structures: the covalent bond, to a finite set of coordinate values, such that with a suitable unit of length can be transformed to give integer values exclusively. These restricted bonds can still be useful for describing real molecular conformations if the minimum magnitude of vector differences is small enough. This can be done, for the example developed here (*PTI* C_α -backbone), using empirical data sampled from molecular dynamics simulations [11], it requires the following steps

1. First we determine the dimensions of the lattice by taking as reference the mean bond length and its range of variation for bonded C_α pairs, in our case this gives: $3.58\text{\AA} < 3.86\text{\AA} < 4.13\text{\AA}$. We set arbitrarily the bond mean length to 20 lattice units, which gives a lattice spacing of 0.19\AA . Thus, any segment between two lattice points with a length range between $3.58 \times 20/3.86$ and $4.13 \times 20/3.86$ is potentially a C_α - C_α bond segment, and the set B of valid **lattice bond segments**, modulo a lattice translation along the x , y and z axes, is the set of segments starting at the origin and ending in any lattice point that lies between two spheres of radius $3.58 \times 20/3.86$

and $4.13 \times 20/3.86$ respectively. This gives a total of 1883 primary segments, excluding reflections through the xy , xz and yz planes.

2. Next we determine the range of variation for the bond angles, which is greater than that for the bond length and varies considerably along the C_α chain. For each bond angle $A_{\alpha_i, \alpha_{i+1}, \alpha_{i+2}}$ we determine two integer numbers : the floored minimum $\lfloor \min(A_{\alpha_i, \alpha_{i+1}, \alpha_{i+2}}) \rfloor$ and the ceiled maximum range $\lceil \max(A_{\alpha_i, \alpha_{i+1}, \alpha_{i+2}}) \rceil$ respectively. These divide the interval between the absolute minimum and maximum values $71^\circ - 167^\circ$ in 64 subintervals

$$\begin{aligned} &71^\circ-74^\circ-75^\circ-76^\circ-77^\circ-78^\circ-79^\circ-80^\circ-81^\circ-82^\circ-87^\circ-89^\circ- \\ &90^\circ-92^\circ-93^\circ-94^\circ-95^\circ-96^\circ-97^\circ-98^\circ-99^\circ-100^\circ-101^\circ- \\ &104^\circ-105^\circ-106^\circ-107^\circ-108^\circ-109^\circ-110^\circ-112^\circ-113^\circ- \\ &114^\circ-115^\circ-116^\circ-117^\circ-118^\circ-119^\circ-120^\circ-121^\circ-124^\circ- \\ &125^\circ-127^\circ-129^\circ-135^\circ-136^\circ-138^\circ-139^\circ-143^\circ-144^\circ- \\ &147^\circ-148^\circ-149^\circ-150^\circ-151^\circ-152^\circ-153^\circ-154^\circ-155^\circ- \\ &156^\circ-157^\circ-159^\circ-162^\circ-163^\circ-167^\circ \end{aligned} \quad (2)$$

3. The dynamic values of each $A_{\alpha_i, \alpha_{i+1}, \alpha_{i+2}}$ spann a given range of intervals from (2), thus consecutive bonds B_α and $B_{\alpha+1}$ can only be assigned discrete bond segments that form an angle within the specific range.

In building realistic 3D-conformations from the DPS s by embedding these in a bigger lattice, the following problem arises: the intervals $C_{\alpha_i} - C_{\alpha_{i+1}}$ between consecutive C_α s, for a given coordinate in Fig. 2, must be replaced by lattice intervals which are generally longer, so the excess lattice units must be distributed among the intermediate sequence intervals, such that the resulting lattice segments bonding C_α s are from the set of valid lattice bond segments described above.

To solve this problem the following steps are needed

1. build from the DPS s the consecutive C_α intervals poset (Fig. 3),
2. determine for each consecutive C_α interval the maximum an minimum excess values,
3. make the linear inequalities in x , y and z independent of one another.

3. The consecutive C_α intervals poset

Fig. 2 shows the DPS s for the PTI C_α -backbone, it also shows some of the intervals between consecutive C_α s : $\mathcal{I}_{\alpha_s}^c$ ³, a partial order relation can be defined for them. But first, we recall some basic definitions : let $\mathcal{I}_{\alpha_1}^c$ and $\mathcal{I}_{\alpha_2}^c$ be two $\mathcal{I}_{\alpha_s}^c$ spanning the DPS_c intervals $\{\sigma_{\alpha_1}^{c_{left}}, \sigma_{\alpha_1}^{c_{right}}\}$ and $\{\sigma_{\alpha_2}^{c_{left}}, \sigma_{\alpha_2}^{c_{right}}\}$

Definition 1 $\mathcal{I}_{\alpha_1}^c$ **precedes** $\mathcal{I}_{\alpha_2}^c$ or $\mathcal{I}_{\alpha_1}^c \prec \mathcal{I}_{\alpha_2}^c$,
if $\mathcal{I}_{\alpha_1}^c \subset \mathcal{I}_{\alpha_2}^c$ or equivalently $\sigma_{\alpha_1}^{c_{left}} \geq \sigma_{\alpha_2}^{c_{left}}$ and $\sigma_{\alpha_1}^{c_{right}} \leq \sigma_{\alpha_2}^{c_{right}}$.

Definition 2 $\mathcal{I}_{\alpha_2}^c$ **succeeds** $\mathcal{I}_{\alpha_1}^c$ or $\mathcal{I}_{\alpha_2}^c \succ \mathcal{I}_{\alpha_1}^c$.

Definition 3 A **maximal** interval is not succeeded by any other interval.

Definition 4 A **minimal** interval is not preceded by any other interval.

Fig. 2 shows the set of maximal intervals for DPS_x , DPS_y and DPS_z .

Definition 5 A **cover** is a set of two intervals $\mathcal{I}_{\alpha_1}^c \prec \mathcal{I}_{\alpha_2}^c$ with no $\mathcal{I}_{\alpha_x}^c$ such that $\mathcal{I}_{\alpha_1}^c \prec \mathcal{I}_{\alpha_x}^c \prec \mathcal{I}_{\alpha_2}^c$.

³The following naming convention applies to any symbol refering to a bond interval $C_\alpha - C_{\alpha+1}$: it bears only the smaller index.

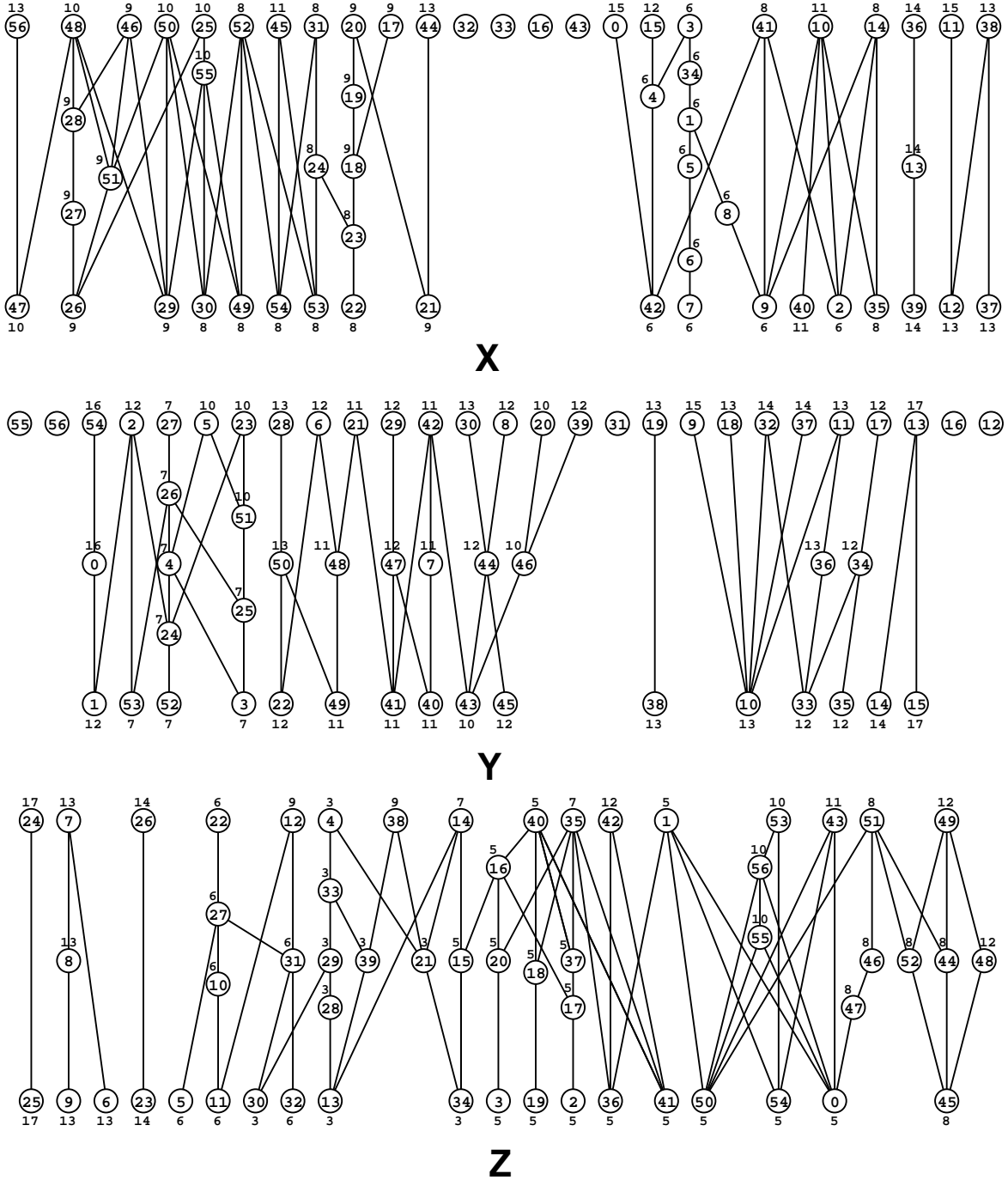


Figure 3: Consecutive C_α intervals cover graph. Minimal/maximal intervals are at the bottom/top respectively, with succession going from bottom to top. For each interval

Fig. 3 displays a graphical representation of this partially ordered set (**poset**), where the nodes are the \mathcal{I}_α^c set and the edge set consists of the pairs satisfying the cover relation. As we shall see below the poset structure allows to define the set of linear inequalities for determining the lattice bond segments.

4. Determining the bounds on excess values

The excess value of an interval \mathcal{I}_α^c is the difference between its length on the *DPS* and on the extended lattice. In order to expand the *DPS* lattice we must determine first the bounds of excess values for every \mathcal{I}_α^c .

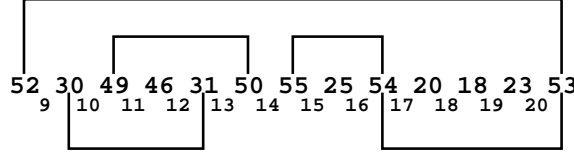


Figure 4: Sequence of maximal interval \mathcal{I}_{52}^x showing its minimal preceeding intervals.

An example will help to understand, we have in Fig. 4 a set of 5 connected \mathcal{I}_α^x s: \mathcal{I}_{52}^x which is a maximal interval, and its minimal predecessors \mathcal{I}_{30}^x , \mathcal{I}_{49}^x , \mathcal{I}_{54}^x and \mathcal{I}_{53}^x (Fig. 3), they fill positions 8 to 20 in the x -sequence where the 12 minimal intervals between C_α s have local excess variables χ_9^x to χ_{20}^x (Fig. 4), giving the local expansion value in the extended lattice. The following equations define the excess values

$$\begin{aligned} X_{52}^x &= \sum_{9 \leq \sigma \leq 20} \chi_\sigma^x - |\mathcal{I}_{52}^x| \quad (\text{where the last term is the } c\text{-sequence interval length}) \\ X_{30}^x &= \sum_{10 \leq \sigma \leq 12} \chi_\sigma^x - |\mathcal{I}_{30}^x| & X_{49}^x &= \sum_{11 \leq \sigma \leq 13} \chi_\sigma^x - |\mathcal{I}_{49}^x| \\ X_{54}^x &= \sum_{15 \leq \sigma \leq 16} \chi_\sigma^x - |\mathcal{I}_{54}^x| & X_{53}^x &= \sum_{17 \leq \sigma \leq 20} \chi_\sigma^x - |\mathcal{I}_{53}^x| \end{aligned} \quad (3)$$

also X_{52}^x must be greater that the sum of the X_α^x from preceeding non-overlapping intervals

$$X_{52}^x \geq X_{49}^x + X_{54}^x + X_{53}^x \quad X_{52}^x \geq X_{30}^x + X_{54}^x + X_{53}^x \quad (4)$$

To build from (4) a complete system of linear inequalities allowing to calculate the χ_σ^c s for embedding the molecular system in the extended lattice, first we need to determine the bounds

$$Xmin_\alpha^c \leq X_\alpha^c \leq Xmax_\alpha^c \quad (5)$$

By construction the maximum lattice bond segment length on any coordinate is 21, this gives for the extreme values of excess lattice units on any interval \mathcal{I}_α^c the relation

$$0 \leq |\mathcal{I}_\alpha^c| + X_\alpha^c \leq 21 \quad (6)$$

which settles the initial minimum and maximum bond lattice units for the c -coordinate to

$$b_c^{min} = 0 \quad \text{and} \quad b_c^{max} = |\mathcal{I}_\alpha^c| + 21 \quad (7)$$

respectively. Let $B_c^{\{b_c^{min}, b_c^{max}\}}$ be the set of all lattice bond segments b such that $b_c^{min} \leq b_c \leq b_c^{max}$ for $c \in \{x, y, z\}$, then the set $B_{\mathcal{I}_\alpha}$ of all the lattice bond segments that are within the bounds (7) is

$$B_{\mathcal{I}_\alpha} = B_x^{\{b_x^{min}, b_x^{max}\}} \cap B_y^{\{b_y^{min}, b_y^{max}\}} \cap B_z^{\{b_z^{min}, b_z^{max}\}} \quad (8)$$

This operation may change the bounds (7), this is because the $b \in B_{\mathcal{I}_\alpha}$ have a common origin but the points at the other extreme form a connected irregular cluster (see the example in Fig. 5): the bonds excluded by (8) may be the ones that contain the extremes of other coordinates. This gives a new set of bonds and the process has to be repeated until the bounds stabilize.

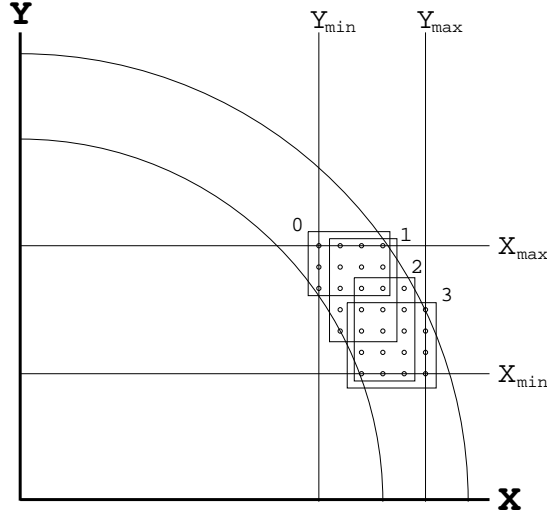


Figure 5: 2D example of a $B_{\mathcal{I}_\alpha}$ set. The lattice bond segments (b) start at the origin, and end on any lattice point in the region bounded by the two spheres described in section 2.1. The only b end points shown are those lying within the x and y bounds, or equivalently $b \in B_{\mathcal{I}_\alpha}$. As shown in the picture the set $B_{\mathcal{I}_\alpha}$ can be decomposed into the minimal covering set of $n_p = 4$ rectangular subsets $\mathcal{P}_{\mathcal{I}_\alpha}^0, \mathcal{P}_{\mathcal{I}_\alpha}^1, \mathcal{P}_{\mathcal{I}_\alpha}^2$ and $\mathcal{P}_{\mathcal{I}_\alpha}^3$.

5. Making the inequalities independent

From the set of bounds (7) we can build the set of linear inequalities (using again the example from the previous section)

$$\begin{aligned}
 Xmax_{52}^x &\geq \sum_{9 \leq \sigma \leq 20} \chi_\sigma^x \geq Xmin_{52}^x \\
 Xmax_{30}^x &\geq \sum_{10 \leq \sigma \leq 12} \chi_\sigma^x \geq Xmin_{30}^x & Xmax_{49}^x &\geq \sum_{11 \leq \sigma \leq 13} \chi_\sigma^x \geq Xmin_{49}^x \\
 Xmax_{54}^x &\geq \sum_{15 \leq \sigma \leq 16} \chi_\sigma^x \geq Xmin_{54}^x & Xmax_{53}^x &\geq \sum_{17 \leq \sigma \leq 20} \chi_\sigma^x \geq Xmin_{53}^x
 \end{aligned} \tag{9}$$

There is a further problem to be taken into consideration: $Xmin_\alpha^c$ and $Xmax_\alpha^c$ are the c -coordinate bounds of the set $B_{\mathcal{I}_\alpha}$, but, due to the non-uniform shape of $B_{\mathcal{I}_\alpha}$, selecting one or more c -values in this interval while discarding the rest may change completely the bounds in the other coordinates. This induces an interdependence between inequalities (9) in x , y and z , in which case solving the system becomes much more complex.

This problem can be avoided if the end points of bonds in $B_{\mathcal{I}_\alpha}$ fill completely a lattice rectangular parallelepiped, in this case the choice of bounds in one coordinate leaves the others unchanged. Thus $B_{\mathcal{I}_\alpha}$ has to be decomposed into a set of rectangular parallelepipeds $\mathbf{P}_{\mathcal{I}_\alpha}$

$$B_{\mathcal{I}_\alpha} = \bigcup_{0 < p \leq n_p} \mathcal{P}_{\mathcal{I}_\alpha}^p, \quad \mathcal{P}_{\mathcal{I}_\alpha}^p \in \mathbf{P}_{\mathcal{I}_\alpha} \tag{10}$$

subject to the following conditions

1. there are no $\mathcal{P}_{\mathcal{I}_\alpha}^{p_1} \in \mathbf{P}_{\mathcal{I}_\alpha}$ and $\mathcal{P}_{\mathcal{I}_\alpha}^{p_2} \in \mathbf{P}_{\mathcal{I}_\alpha}$ such that $\mathcal{P}_{\mathcal{I}_\alpha}^{p_1} \subset \mathcal{P}_{\mathcal{I}_\alpha}^{p_2}$,
2. n_p is minimal,
3. for $\mathbf{P}_{\mathcal{I}_\alpha}$ obeying conditions 1 and 2 and $\mathcal{P}_{\mathcal{I}_\alpha}^{p_1} \in \mathbf{P}_{\mathcal{I}_\alpha}$ there is no $\mathcal{P}_{\mathcal{I}_\alpha}^{p_2}$ such that $|\mathcal{P}_{\mathcal{I}_\alpha}^{p_1}| < |\mathcal{P}_{\mathcal{I}_\alpha}^{p_2}|$.

In that case striking the bounds of a set $\mathcal{P}_{\mathcal{I}_\alpha}^p$ for any coordinate does not alter the bounds in the other dimensions and thus solutions to the inequalities can be found independently for each coordinate.

6. The structure of the solutions

The inequalities (9), for instance, can be rewritten as

$$Xmax_{52} \geq U_{9,20} \cdot \chi^x \geq Xmin_{52} \quad \dots \quad (11)$$

where the $U_{\mathcal{I}_\alpha}$ s are $(N-1)$ -dimensional vectors of the form

$$U_{\mathcal{I}_\alpha} = (0, \dots, 0, 1, \dots, 1, 0, \dots, 0) \quad (12)$$

with ones in the contiguous positions from σ_α^{cleft} to σ_α^{cright} and zeros everywhere else, and χ^x is the vector

$$\chi^x = (\chi_0^x, \dots, \chi_9^x, \dots, \chi_{20}^x, \dots, \chi_{N-1}^x) \quad (13)$$

Extending this notation to the whole set of inequalities for $0 \leq \alpha \leq N-1$ and x, y and z , we have

$$\begin{aligned} Xmax_{\mathcal{I}_\alpha}^x &\geq U_{\mathcal{I}_\alpha}^x \cdot \chi^x \geq Xmin_{\mathcal{I}_\alpha}^x \\ Xmax_{\mathcal{I}_\alpha}^y &\geq U_{\mathcal{I}_\alpha}^y \cdot \chi^y \geq Xmin_{\mathcal{I}_\alpha}^y \\ Xmax_{\mathcal{I}_\alpha}^z &\geq U_{\mathcal{I}_\alpha}^z \cdot \chi^z \geq Xmin_{\mathcal{I}_\alpha}^z \end{aligned} \quad (14)$$

Taking the vectors $U_{\mathcal{I}_\alpha}$ as the rows of a $(N-1) \times (N-1)$ matrix U^c , and $Xmax_{\mathcal{I}_\alpha}^c / Xmin_{\mathcal{I}_\alpha}^c$ as the components of vectors $Xmax^c / Xmin^c$ (14) can be rewritten as

$$Xmax^x \geq U^x \cdot \chi^x \geq Xmin^x \quad Xmax^y \geq U^y \cdot \chi^y \geq Xmin^y \quad Xmax^z \geq U^z \cdot \chi^z \geq Xmin^z \quad (15)$$

The above set of inequalities define $2 \times (N-1)$ affine half-spaces $Hmin_{\mathcal{I}_\alpha}^c$ and $Hmax_{\mathcal{I}_\alpha}^c$ whose intersection determines an H-polytope in CS^c [12, 13]. Hence, the vertices of this polytope are among the unique solutions of the $3 \times 2^{N-1}$ systems of equations

$$U^x \cdot \chi^x = Xlim^x \quad U^y \cdot \chi^y = Xlim^y \quad U^z \cdot \chi^z = Xlim^z \quad 0 \leq \alpha \leq N-1 \quad (16)$$

where $Xlim^c$ can be either $Xmax^c$ or $Xmin^c$ and the \geq relation in (15) has been restricted to $=$. Moreover, the matrices U^c with rows like (12) are called **interval matrices**, they belong to a very important class of matrices called: **totally unimodular matrices** [12]. These have the particularity that the determinant of any minor is either $-1, 0$ or 1 . This ensures that the vertices of the polytope are integer vectors (or lattice points), since solving (16) by applying the Cramer's rule the denominator is always -1 or 1 . Thus, the solutions of (16) can be written

$$\chi^c = \overline{U}^c \cdot Xlim^c \quad (17)$$

where \overline{U}^c is the inverse of U^c .

The V-polytope is the representation of the polytope by its set of vertices, these can be obtained from (17) by determining the combinations in $Xlim^c$ compatible with (15). The solutions of the system of linear inequalities (15) can be generated from this set through convex combinations, as the three sets of inequalities are independent the general solution will be the product of the x, y and z polytopes.

The total unimodularity of matrix U^c also ensures that most combinatorial algorithms can be run in polynomial time.

7. Conclusion

The purpose of the line of work being developped here, is to show that molecular structures can be built and analysed with a fraction of the information (in our case less than 1/5) that can be found in a typical PBD file.

This might seem a significant but modest quantitative difference, but qualitatively is more than that: discarding information results in the emergence of mathematical structures that were buried in the complexity of the data, which in turn can be encoded efficiently by them. Using combinatorics a great number of molecular conformations can be dealt simultaneously, thus overcoming the barrier that computations have to be performed on the basis of one conformation at a time.

The algorithmic method developped before [1 – 5] serves two purposes

1. As an **amplifier** : by codifying data sampled in computer simulations into discrete geometrical structures, these can be combined to generate an estimate of the volume occupied by a molecule in its conformational space.
2. As a molecular 3D-structure **compressor** : it is possible to translate basic features of molecular 3D-structures into a binary code, which in turn can be very efficiently amalgamated into ternary sequences that encode great numbers of cells from *CS*. The information on the whole *CS* volume can be cast into a file compatible with desktop memory size.

The present work is the first one of a third and last step: the development of combinatorial methods for calculating the energy of structures from cells in *CS*.

Here we have developped the basic algorithms for this : realistic discrete protein conformations can be built and embedded in a cubic lattice, using a table of discrete bond segments and, more important, these conformations can be encoded into combinatorial structures.

However many issues still remain unexplored:

- The possible combinations of $\mathcal{P}_{\mathcal{I}_\alpha}^p$ s from (10) is a huge set, efficient sampling methods should be developped.
- The V-polytope should be better characterized.
- The present formalism should be extended to take into account sets of adjacent cells.
- Last of all inter-atomic distances should also be encoded into combinatorial structures.

These will be dealt in forthcoming works.

8. Appendix

Table 1. Lattice coordinates of the *PTI* C_α -backbone from Fig. 1.

Column α : C_α number.

Columns x_α y_α z_α : C_α coordinates.

Columns b_x b_y b_z : bond vector between $C_{\alpha-1}$ and C_α .

α	x_α	y_α	z_α	b_x	b_y	b_z	α	x_α	y_α	z_α	b_x	b_y	b_z
0	0	0	0				29	-34	49	-30	6	19	7
1	19	7	1	19	7	1	30	-33	66	-40	1	17	-10
2	30	5	-16	11	-2	-17	31	-25	84	-38	8	18	2
3	31	26	-19	1	21	-3	32	-9	94	-44	16	10	-6
4	12	26	-26	-19	0	-7	33	-1	113	-41	8	19	3
5	19	19	-43	7	-7	-17	34	14	111	-29	15	-2	12
6	28	35	-49	9	16	-6	35	30	123	-29	16	12	0
7	19	52	-53	-9	17	-4	36	38	117	-12	8	-6	17
8	27	68	-45	8	16	8	37	55	106	-15	17	-11	-3
9	29	86	-53	2	18	-8	38	64	91	-25	9	-15	-10
10	28	106	-48	-1	20	5	39	50	80	-34	-14	-11	-9
11	47	105	-41	19	-1	7	40	44	61	-30	-6	-19	4
12	60	120	-46	13	15	-5	41	36	55	-13	-8	-6	17
13	54	131	-31	-6	11	15	42	17	51	-19	-19	-4	-6
14	40	145	-33	-14	14	-2	43	12	69	-11	-5	18	8
15	24	141	-21	-16	-4	12	44	-3	68	2	-15	-1	13
16	6	137	-29	-18	-4	-8	45	-14	83	12	-11	15	10
17	-3	126	-15	-9	-11	14	46	-32	75	11	-18	-8	-1
18	-15	111	-21	-12	-15	-6	47	-44	65	-1	-12	-10	-12
19	-8	93	-14	7	-18	7	48	-50	50	10	-6	-15	11
20	-16	76	-19	-8	-17	-5	49	-33	46	18	17	-4	8
21	-7	60	-28	9	-16	-9	50	-24	47	0	9	1	-18
22	-13	42	-32	-6	-18	-4	51	-38	32	-4	-14	-15	-4
23	-15	41	-52	-2	-1	-20	52	-34	23	13	4	-9	17
24	-10	22	-57	5	-19	-5	53	-15	22	9	19	-1	-4
25	-18	25	-75	-8	3	-18	54	-17	18	-11	-2	-4	-20
26	-36	29	-67	-18	4	8	55	-24	-1	-8	-7	-19	3
27	-35	17	-51	1	-12	16	56	-36	-12	3	-12	-11	11
28	-40	30	-37	-5	13	14	57	-52	-15	-9	-16	-3	-12

References

- [1] **A central partition of molecular conformational space. I. Basic structures.**
J. Gabarro-Arpa, *Comp. Biol. & Chem.* **27**, 153-159 (2003).
- [2] **A central partition of molecular conformational space. II. Embedding 3D structures.**
J. Gabarro-Arpa, *Proceedings of the 26th Annual International Conference of the IEEE EMBS, San Francisco*, 3007-3010 (2004).
- [3] **A central partition of molecular conformational space. III. Combinatorial determination of the volume spanned by a molecular system in conformational space.**
J. Gabarro-Arpa, *J. Math. Chem.* **42**, 691-706 (2006).
- [4] **A central partition of molecular conformational space. IV. Extracting information from the graph of cells.**
J. Gabarro-Arpa, *J. Math. Chem.* **44**, 872-883 (2006).
- [5] **A central partition of molecular conformational space. V. The Hypergraph of 3D Partition Sequences.**
J. Gabarro-Arpa
arXiv:0812.2844 (2008).
- [6] **Energy landscapes.**
D.J. Wales, Cambridge University Press, ISBN 0-521-81415-4, (2003).
- [7] **Dynamic personalities of proteins.**
K. Henzler-Wildman, D. Kern, *Nature* **450**, 964-972 (2007).
- [8] **All-atom empirical potential for molecular modeling and dynamics studies of proteins.**
A.D. MacKerell Jr., et al., *J. Phys. Chem. B* **102**, 3586-3616 (1998).
- [9] **Biomolecular simulations: recent developments in force fields, simulations of enzyme catalysis, protein-ligand, protein-protein, and protein-nucleic acid noncovalent interactions.**
W. Wang, O. Donini, C.M. Reyes, P.A. Kollman
Annu. Rev. Biophys. Biomol. Struct. **30**, 211-243 (2001).
- [10] **The geometry of the reactive site and of the peptide groups in trypsin, trypsinogen and its complexes with inhibitors.**
M. Marquart, J. Walter, J. Deisenhofer, W. Bode, R. Huber
Acta Crystallogr. Sect. B **39**, 480-490 (1983).
- [11] **Clustering of a molecular dynamics trajectory with a Hamming distance.**
J. Gabarro-Arpa, R. Revilla, *Comput. Chem.* **24**, 693-698 (2000).
- [12] **Theory of Linear and Integer Programming.**
A. Schrijver, John Wiley & sons, ISBN 0-471-98232-6, pp. 155-156 (1998).
- [13] **Lattice points and lattice polytopes.**
A. Barvinok, *Handbook of Discrete and Computational Geometry*, CRC Press, ISBN 0-8493-8524-5, pp. 133-152 (1997).